NON-ZEEMAN CIRCULAR POLARIZATION OF MOLECULAR SPECTRAL LINES IS COMMON IN STAR-FORMING REGIONS

M. A. CHAMMA[1], M. HOUDE[1], J. M. GIRART[2] AND R. RAO[3]

[1]Department of Physics and Astronomy, The University of Western Ontario, London, ON, N6A 3K7, Canada

[2]Institut de Ciències de l'Espai (IEEC-CSIC), Can Magrans, S/N, E-08193 Cerdanyola del Vallès, Catalonia, Spain

and

[3]Submillimeter Array, Academia Sinica Institute of Astronomy and Astrophysics, 645 N. Aohoku Place, Hilo, HI 96720, USA

Abstract

Understanding the magnetic field in star-forming regions allows us to test ideas about free-fall collapse and support mechanisms in molecular clouds, filling in details about the star formation process. These magnetic fields are usually probed through linear polarization observations from dust continuum and molecular spectral transitions and analysed through the Davis-Chandrasekhar-Fermi method. For molecular lines circular polarization is usually ignored, largely because of difficulty in measurement and its assumed irrelevance. We find in archival data of the Submillimeter Array (SMA) several examples of circular polarization in common molecular tracers, most notably CO. This circular polarization possibly arises from anisotropic resonant scattering implying that some background linearly polarized flux is being converted and lost to circular polarization. We find circular polarization in NGC7538, IRC+10216 and Orion KL to sufficient degrees that we believe the presence of circular polarization in these spectral lines is widespread for such objects, implying that an important piece of information has been missed when studying magnetic fields through linear polarization from molecular spectral lines in star-forming regions.

1. INTRODUCTION

This section will cover the background of measuring magnetic fields in star-forming regions and Section 2 will discuss the issues that arise when doing polarimetry with radio interferometry, focusing specifically on circular polarization (CP). Section 3 presents archival observations of four objects made with the Submillimeter Array (SMA) on Mauna Kea and makes the case that these circular polarization detections are real and physical. Section 4 will give in detail our scheme for correcting a spurious source of CP that arises with the SMA. Finally in Section 5 we'll highlight the significance of these CP detections and summarize relevant research.

Since we can only measure the light from star-forming regions astronomers use polarimetry to infer properties like the direction and magnitude of the magnetic field. The Davis-Chandrasekhar-Fermi is one method that uses the dispersion of polarization angles in the thermal emission of dust to find the magnitude and direction of the plane-of-the-sky component of the magnetic field. The presence of a magnetic field leads to linearly polarized radiation because dust grains will align themselves to the field. This aligned dust emits thermal radiation in the continuum that is linearly polarized (J. P. Vallée 2011). Aligned dust will also absorb radiation whose polarization is aligned with its long axis, acting as a sort of polarizing grid. Thus measuring the amount of linear polarization in the infrared continuum tells us about the degree to which the dust is aligned with the magnetic field which in turn tells us about the strength of the magnetic field.

In addition to this technique the interaction between certain molecules and the ambient magnetic field can cause that molecule's transitions to be linearly polarized by a few percent through the Goldreich-Kylafis effect. The amount of linear polarization in the spectral line can be measured and used to infer properties of the magnetic field.

A significant amount of unexpected circular polarization was reported by Houde et al. (2013) in a rotational transition of CO using the Caltech Submillimeter Observatory (CSO), a common tracer of the magnetic field. The presence of circular polarization in a molecular transition is usually explained with Zeeman splitting, but the lines of CO only split at magnetic fields of several thousand gauss. In addition, the observed Stokes V profile

was positive and symmetric, which is also unexpected since Zeeman splitting gives rise to an antisymmetric Stokes V profile. To explain this detection a model was proposed whereby linearly polarized light is converted to circularly polarized light through anisotropic resonant scattering (ARS) (Houde et al. 2013; Houde 2014). This was tested in IC443 by Hezareh et al. (2013) where the measured circularly polarized flux of a CO line was 're-added' into the measured linearly polarized flux to correct the polarization angles. They found that the polarization angles obtained from the CO tracer only agreed with those obtained from dust polarimetry after the circularly polarized flux was accounted for. If ARS is common to other objects then using CO as a tracer of the magnetic field will have a systematic error unless the circular polarization of CO's lines are also measured. The goal of this paper is to show several examples of such circular polarization.

2. MEASUREMENT OF CIRCULAR POLARIZATION WITH RADIO INTEROFEROMETRY

The measurement of circular polarization in the radio is challenging to calibrate, especially when using radio interferometers like the SMA or ALMA. The SMA polarimeter uses a quarter-waveplate (QWP) to convert incident linearly polarized light to circular primarily to measure linear polarization. While not its intended use, The QWP can work the other way to measure CP: incident CP is converted to LP and then measured by the receivers. ALMA on the other hand uses linear feeds and measures the linearly polarized light directly. While both types of feeds can be used to measure circular polarization, the calibration process is different Sault et al. (1996). Currently ALMA does not support measuring Stokes V reliably. The SMA has been used to take precise measurements of CP in Sgr A* as reported in Muñoz et al. (2012). For a discussion on measuring CP with radio interferometry and on design choices at the SMA (such as the choice of converting from linear- to circular-polarization and vice-versa) see Hamaker et al. (1996); Marrone et al. (2008).

3. OBSERVATIONS

We collected radio interferometric archival polarimetry observations from the Submillimeter Array (SMA) archive that had been measured using the circular feeds, a similar setup to that used by Muñoz et al. (2012) to measure circular polarization in Sgr A*. Because the archival observations were not taken with measurements of circular polarization in mind the SNR is often very low, and we had to average velocity channels to increase the SNR at the cost of spectral resolution. This generally increases the SNR from 3-4 to 6-10.

The four objects we present here are Orion KL, NGC7538, NGC1333 and IRC+10216. The first three are well-known star-formation regions while IRC+10216 is an evolved carbon star. We find significant Stokes V signals in all objects except for NGC1333. The visibility data are corrected for beam squint, an instrumental artifact that gives rise to spurious Stokes V signals. Squint gives rise to distinct pairs of positive and negative peaks of Stokes V throughout the inverted image. Maps are then made of the continuum and lines for each object. The squint correction is confirmed visually by inspecting the Stokes V maps, where we see the pairs of peaks largely disappear. More details on the squint correction will be given in the next section.

Figure 1 shows corrected Stokes I and Stokes V spectra obtained at the peak of Stokes V on the corresponding maps. A comparison of Stokes V spectra before and after correction are shown in Figure 4. Notice in all cases the Stokes V signal decreases after squint correction. Stokes V can be found in the average of all the visibility data as well, though the significance is 3-5σ in that case compared to approximately 6-10σ when the spectra is taken from the inverted maps. We present here only the map spectra. In general the peaks of Stokes I and Stokes V do not align in the maps.

In Orion KL the lines of CO ($J = 3 \rightarrow 2$ at 345.8GHz) and SiO ($J = 8 \rightarrow 7$ at 347.3GHz) are both bright (peak Stokes I of around 20 Jy/beam and 55 Jy/beam respectively; not shown) and both show Stokes V signals. The CO Stokes V signal has an antisymmetric structure while the SiO Stokes V signal is purely negative. Figure 3 shows the peak Stokes V signal of the SiO line. We checked the average of all the visibilities (average over all antennae baselines and all time intervals) and found that the CO Stokes V signal is more intense than the SiO Stokes V signal, and the Stokes I intensities after averaging the visibilities were approximately 50 Jy and 75 Jy for CO and SiO respectively. If the Stokes V signal were purely leakage from Stokes I than we would expect to see an SiO Stokes V signal that is stronger than the CO Stokes V signal, but we do not.

In IRC+10216 we again see Stokes V in the CO transition at 345.8 GHz but also several signals in CS, SiS, and H^{13}CN. These lines and their frequencies are listed in Table 2. We again note that the Stokes I intensity is not proportional to the Stokes V intensity. The detection in CS at 342.8 GHz is huge compared to it's I intensity.

In NGC7538 there was a strong Stokes V detection in CH$_2$CO at 346.6 GHz that completely disappeared after correction. The Stokes V signal in CO at 345.8 GHz decreased in intensity but is still extremely prominent.

Finally Figure 2 shows no detection in NGC1333, with only a weak detection of CO in Stokes I.

Object	Coordinates (J2000)	Array Configuration	Date Observed
Orion KL	RA 05$^{\rm h}$35$^{\rm m}$14.501$^{\rm s}$ Dec -05°22'30.40"	Compact	2008-01-06
NGC7538	RA 23$^{\rm h}$13$^{\rm m}$44.771$^{\rm s}$ Dec +61°26'48.85"	Compact	2014-10-28
IRC+10216	RA: 09$^{\rm h}$47$^{\rm m}$57.381$^{\rm s}$ Dec +13°16'43.70"	Compact	2009-11-24
NGC1333	RA 03$^{\rm h}$28$^{\rm m}$55.580$^{\rm s}$ Dec +31°14'37.10"	Compact	2010-10-14

Table 1. Summary of Archival Observations Used

When assessing the Stokes V detection we consult the map for obvious pairs of positive/negative peaks that would indicate beam offset and therefore a false Stokes V signal. The maps are taken around a very narrow frequency band of around 2 MHz so any peaks that exist shouldn't be washed out by noise in adjacent channels. In the maps for Orion KL and IRC+10216 shown in Figure 1 there are no negative peaks around the peak of Stokes V. However in NGC7538 there is quite a large negative Stokes V peak near our chosen peak that may indicate squint. The top panel of Figure 5 shows what 'squint peaks' look like (we know these peaks are from squint because they disappear after correction) and the pairs tend to resemble each other in shape. The pair of peaks around our chosen peak in NGC7538 however have distinct shapes. The worst case here is that the signal is entirely squint but on the other hand the signal may be a mixture of real and heavily affected by squint. The detections in Orion KL and IRC+10216 are more reliable.

Table 1 shows a summary of the objects presented and related information.

4. SQUINT CORRECTION

Here we describe spurious Stokes V that arises when using the SMA and our scheme for correcting it. This instrumental Stokes V comes from a slight pointing offset between the left- and right-handed CP beams.

The archival data used was in all cases observed with the goal of measuring linear polarization (i.e., the Stokes Q and Stokes U parameters). On the SMA this is done with a quarter-waveplate placed in front of the linear receivers to convert incident circular polarization (CP) to linear polarization. While this method is relatively imprecise, it avoids having to solve for the linear polarization terms of calibration objects when obtaining Stokes V (Marrone et al. 2008; Thompson et al. 2001). Obtaining Stokes V from the visibilities measured with circular feeds is done as follows. Given antennae a and b,

Object	Line	(GHz)	Stokes V (Jy/beam)
Orion KL	CO $J = 3 \rightarrow 2$	345.78	0.65
	SiO $J = 8 \rightarrow 7$	347.3	-0.65
NGC7538	CO $J = 3 \rightarrow 2$	345.8	0.85
IRC+10216	CS $J = 7 \rightarrow 6$	342.88	0.6
	SiS $J = 19 \rightarrow 18$	344.78	0.2
	H^{13}CN $J = 4 \rightarrow 3$	345.34	0.8
	CO $J = 3 \rightarrow 2$	345.8	0.4
NGC1333 (IRAS2a)	CO $J = 3 \rightarrow 2$	345.8	None

Table 2. Summary of corrected Stokes V signals found. The beam size is determined by the configuration of the antennae array. An intensity for the Stokes V signal is only given if the peak is noticeably higher than the noise level. The intensity quoted for CO in NGC7538 is before smoothing is applied.

the Stokes V visibility in the circular feed case is found through (Muñoz et al. 2012):

$$\mathcal{V}_V \simeq \frac{1}{2}\left\{\mathcal{V}_{RR}/(g_{Ra}g_{Rb}^*) - \mathcal{V}_{LL}/(g_{La}g_{Lb}^*)\right\}$$

Here the right-handed CP and left-handed CP visibilities are $\mathcal{V}_{RR}$ and $\mathcal{V}_{LL}$ and are measured by orienting the quarter-waveplate that is placed in the beam of the antennae. The complex gain factors for each polarization for each antennae are g_{Ra}, g_{Rb}, g_{La} and g_{Lb} with 'R' and 'L' for right- and left-CP, respectively. Because the Stokes V visibility is found by taking the difference of two beams a slight offset gives rise to pairs of positive and negative peaks of Stokes V, as shown in Figure 5. This offset likely arises because of slight differences in the index of refraction of the quarter-waveplate when it is rotated, but hasn't been studied with the SMA as far as we know.

Because the visibilities are the Fourier transform of the intensity map, an offset in image space is equivalent to a complex exponential term in visibility space that can be absorbed into the gain coefficients (see Appendix). Thus it is easiest to correct for the offset in visibility-space by using *Miriad* (citation) to solve for the gain coefficients on each beam. Specifically the process is:

1. Observations are calibrated for gain and phase in the usual way using calibration observations of 'good' sources (usually quasars like 3C84, 3C454, etc.) (See Miriad User Guide Sault et al. (2008))

2. Visibilities are split into line-free continuum data and line data. These are then mapped and used to obtain CLEAN models
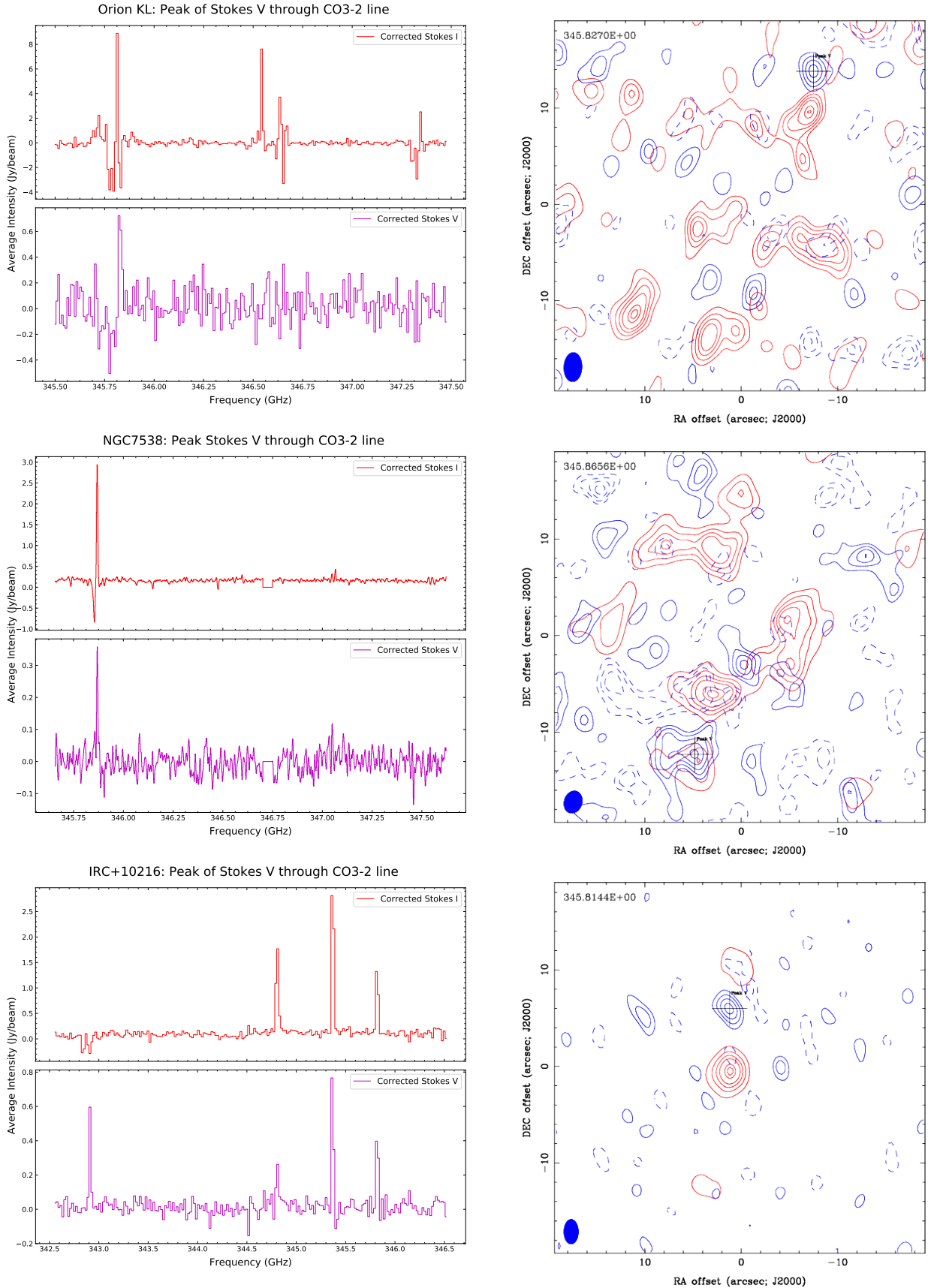
Figure 1. Corrected maps of the CO $J = 3 \rightarrow 2$ line (345.8GHz) and corrected spectra for Orion KL, NGC7538, IRC+10216. **Maps:** Blue contours are Stokes V and are shown at the -4, -3, -2, 2, 3, 4σ levels. The RMS error for each Stokes V map is found using *Miriad's* `imstat` command. Dark red contours are Stokes I and the levels are 15%, 30%, 45%, 60%, 85% and 95% of the maximum. The value in the top left is the frequency of the mapped signal. Each map has a narrow bandwidth of ~2 MHz around the frequency given in the top left corner. **Spectra:** *Miriad's* `maxfit` is used on the CO map to obtain the location on the image where the Stokes V signal at 345.8GHz is maximum, and a spectra is obtained through that point. The cross on the map denotes the location of that peak. The spectrum for NGC7538 is Hanning smoothed by a length of 15.
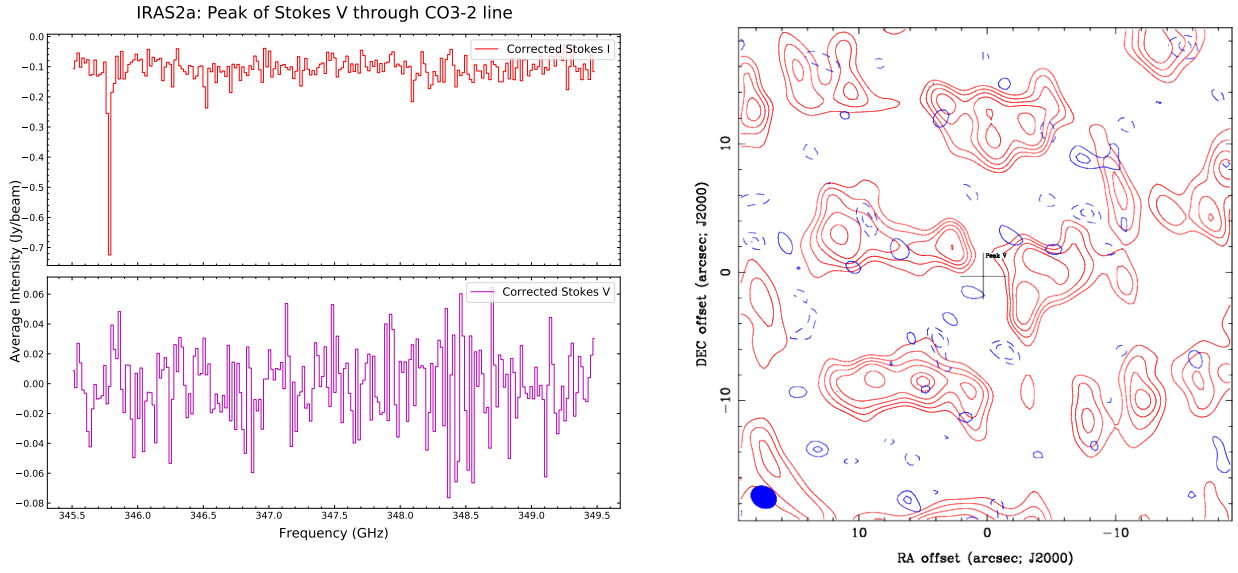
Figure 2. Corrected maps of the CO $J = 3 \rightarrow 2$ line and corrected spectrum for NGC1333 (IRAS2a). No significant Stokes V signal is detected here, probably because the object is too dim. Contours are the same levels as in Figure 1 and the spectrum is obtained the same way.
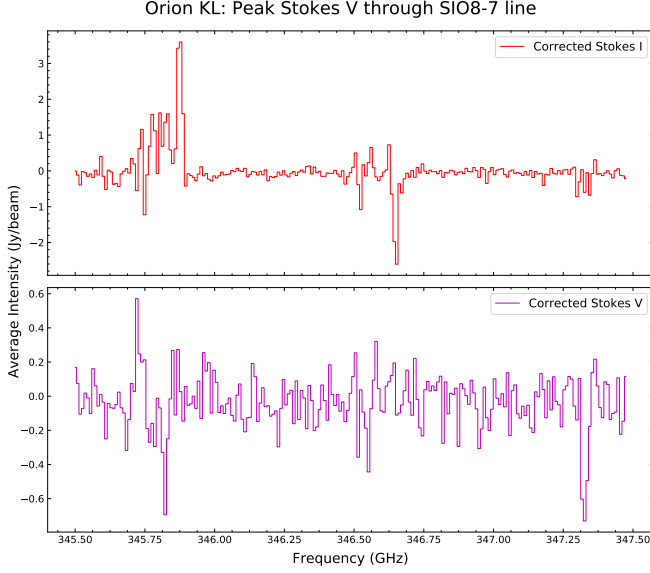
Figure 3. Peak Stokes V signal for the SiO ($J = 7 \rightarrow 8$ at 347.3 GHz) transition in Orion KL. Note there is also a strong Stokes V signal in the CO ($J = 3 \rightarrow 2$ at 345.8 GHz) transition here. The SiO signal is purely negative but the CO signal is antisymmetric.

3. The separate continuum and line data are further split into LL and RR visibilities. *Miriad*'s `self-cal` is used on the continuum data to solve for the gain coefficients of each antenna and each polarization (L or R). This is done by minimizing the difference between measured visibilities $\mathcal{V}_{ij}$ of antennae i and j and model visibilities $\hat{\mathcal{V}}_{ij}$ according to $\epsilon^2 = \sum |\mathcal{V}_{ij} - g_i g_j^* \hat{\mathcal{V}}_{ij}|^2$ for each of the correlations LL and RR (Sault et al. 2008; Schwab 1980). The model visibilities used are those found earlier.

4. The gains found from the continuum LL data is then applied to the line LL data, similarly for the RR continuum and line data.

5. The different polarizations (LL, RR, RL, LR) are recombined and inverted to produce corrected maps. Spectra can be obtained either from the corrected visibilities or the maps.

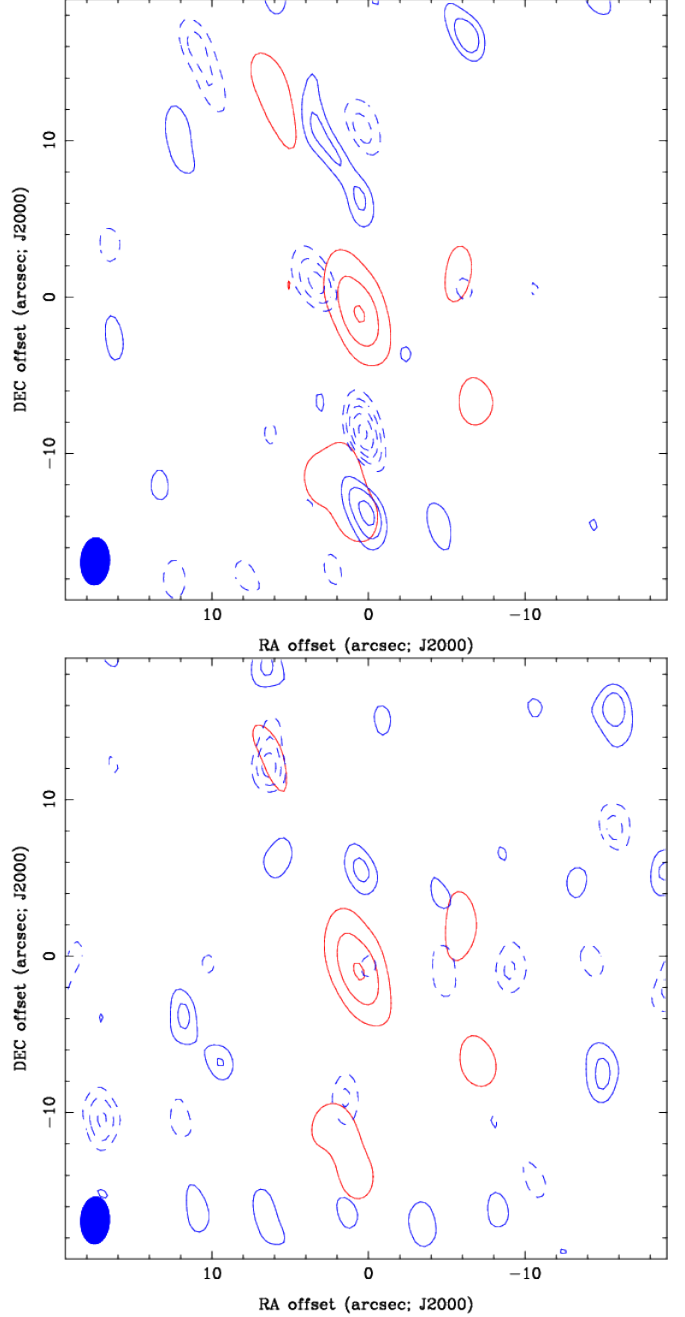Figure 5 shows maps before and after this correction is applied.

Figure 5. Map of the continuum around 345GHz in Orion KL before (top) and after (bottom) squint correction. Red contours are Stokes I, blue contours are Stokes V. Dashed lines denote negative values, solid lines denote positive values. Note the multiple pairs of positive and negative Stokes V peaks. These largely disappear after correction. The contour scales on both maps are identical. Red Stokes I contours are at 15%, 35%, 55%, 75% and 95% of the peak intensity. Blue Stokes V contours are at -8, -7, -6, -5, -4, -3, -2, 2, 3, 4, 5, 6, 7 and 8σ levels.

5. DISCUSSION

Are these detections of CP in CO real and are they as common as these archival observations lead us to believe?

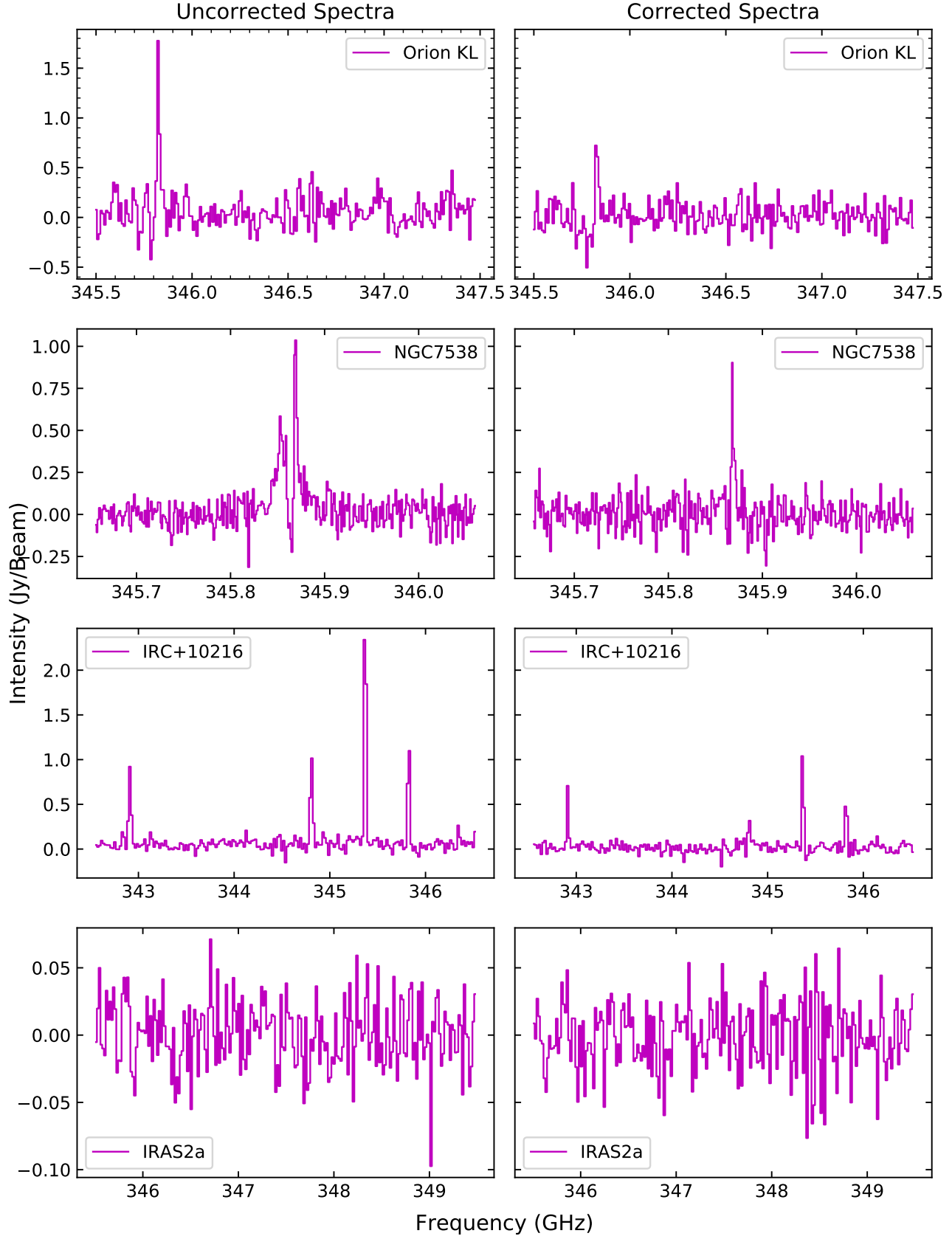# Stokes V Map Spectra before and after squint correction

Figure 4. Stokes V spectra of all objects before and after squint correction. *Miriad*'s `maxfit` is used on the CO map for each respective object to obtain the location in the image where the Stokes V signal at 345.8GHz is maximum, and a spectra is obtained through that point.

- Summarize earlier detections

- Summarize ARS, other theories

5.1. *Linear vs. Circular Feeds*

To illustrate briefly the differences between the two feed types consider the following: with orthogonal circular polarization bases, the Stokes V parameter for a beam of light is defined by $V = \langle E_l^2 \rangle - \langle E_r^2 \rangle$, where E is the electric field vector and l and r correspond to the orthogonal left-CP and right-CP bases. With orthogonal linear bases Stokes V is defined by $V = -2\mathrm{Im}(E_x E_y^*)$ where x and y are the linear bases. In the circular case we take the difference of two measured intensities while the linear feed case requires us to measure the phase of the electromagnetic wave.

Now when the measurement is made with interferometry it is the visibilities –the correlated waveforms between a pair of antennae– that are measured. In the circular case the Stokes V visibility is roughly $\mathcal{V}_V \propto \mathcal{V}_{RR} - \mathcal{V}_{LL}$ where $\mathcal{V}_{RR}$ and $\mathcal{V}_{LL}$ are the visibilities obtained from correlating two antenna measuring right-CP and left-CP respectively. In the linear feed case the Stokes V visibility is coupled with the Stokes Q and U visibilities (Thompson et al. 2001). This means the Stokes Q and U of any calibration object must be measured as well. This is not possible with the SMA setup.

6. CONCLUSION

Sup

REFERENCES

Hamaker, J. P., Bregman, J. D., & Sault, R. J. 1996 A&A Suppl. Ser., 117, 137-147

Hezareh, T. J., Wiesemeyer, H., Houde, M., Gusdorf, A., Siringo, G. 2013 A&A, 558, A45

Houde, M., Hezareh, T., Jones, S., & Rajabi, F. 2013 ApJ, 764, 24

Houde, M. 2014 ApJ, 795, 27

Muñoz, D. J., Marrone, D. P., Moran, J. M., & Rao, R. 2012 ApJ, 745, 115

Marrone D. P. & Rao R. 2008, Proc. SPIE 7020, 70202B

Sault, R. J., Hamaker, J. P., & Bregman, J., D. 1996 A&A Suppl. Ser., 117, 149-159

Sault, R. J., Killeen, N. 2008, Miriad Users Guide, Australia Telescope National Facility

Schwab, F. R. 1980, Proc. SPIE 0231, Intl Optical Computing Conf I

Thompson, A. R., Moran, J. M., & Swenson Jr, G. W. 2001, Interferometry and synthesis in radio astronomy (John Wiley & Sons)

Vallée, J. P. 2011, New Astronomy Reviews 55, 23–90